Supplementary Information

Network of Heterogeneous Catalyst Arrays on the Nitrogen-Doped Graphene for Synergistic Solar Energy Harvesting of Hydrogen from Water

Sang Rim Shin[†], Jung Hyo Park[†], Keon-Han Kim[†], Kyung Min Choi[*,§], and Jeung Ku Kang[*,†,‡]

[†]Department of Materials Science and Engineering and [‡]Graduate School of Energy, Environment, Water, and Sustainability (EEWS), Korea Advanced Institute of Science and Technology (KAIST), 291 Daehak-ro, Yuseong-gu, Daejeon 305-701, Republic of Korea

[§]Department of Chemical and Biological Engineering, Sookmyung Women's University, 100 Cheongpa-ro 47 gil, Yongsan-gu, Seoul 140-742, Republic of Korea

* Corresponding Author: E-mail: kmchoi@sookmyung.ac.kr, jeungku@kaist.ac.kr

■ THE DETAILS FOR MATERIALS CHARACTERIZATION

Scanning electron microscopy (SEM): In the SEM (JEOL, JSM-7600F) measurement, we used a mild electron beam, 0.5 KeV acceleration voltages in the gentle beam mode to avoid structural damage. We observed the morphology of the photocatalysts.

Transmission electron microscopy (TEM) along with the total x-ray reflection fluorescnece (TXRF) spectrometer: The TEM images were collected by JEOL (JEM-ARM200F) Cs-corrected scanning transmission electron microscopy. The TXRF (Nano hunter, Rigaku Corporation, Mo source) elemental analysis was carried out to confirm the components of a structure.

X-ray photoelectron spectroscopy (XPS): The XPS spectra were obtained using a Sigma Probe from Thermo VG Scientific, which is equipped with a 350 W Al anode X-ray source along with a multi-anode, a pulse counting, and a hemispherical analyzer. The spectra were collected using an incident photon energy of 1486.6 eV and were corrected for the detector's work function.

Raman spectroscopy: The defect or distortion of the graphene in the electrode is observed by Raman spectra. Raman spectra were obtained using a high resolution dispersive Raman microscope (ARAMIS, HORIBA), which is equipped by an Ar ion CW Laser (514 nm).

Time-correlated single photon counting (TCSPC) spectrometer: The time-correlated florescence decay spectra at the emission peak of a 520 nm laser were collected by the Edinburgh EPLED-300 to increase the temporal solution of photocatalysts for pico-second fluorescence decays.

■ THE DETAILS FOR CALCULATION OF PHOTOCATALYTIC EFFICIENCY

Quantum yield (QY) calculation: the efficiency for photocatalytic performance has been determined by calculation of the quantum yield based on the following equations of

$$\text{Quantum Yield (\%)} = \frac{\text{Number of reacted electrons}}{\text{Number of incident photons}} \times 100 \qquad \text{Equation (S1)}$$

$$= \frac{2 \times \text{Number of } H_2 \text{ molecules evolved}}{\text{Number of incident photons}} \times 100 \qquad \text{Equation (S2)}$$

$$= \int \frac{2 n_{H_2} N_A h c}{P_\lambda \lambda_s t} \, d\lambda \times 100 \qquad \text{Equation (S3)}$$

where n_{H_2} is the amount of hydrogen evolved over the light exposure time of t, N_A is Avogadro's constant, h is Planck's constant, c is the speed of the light, P_λ is the output power of the incident light at each wavelength of λ_s. It is notable that the relative portion of the light at a certain wavelength of λ_s was calculated, and multiplied with the light intensity 150 mW/cm^2 used in the experiment to deriveP_λ. Then, the total numbers of incident photons were determined by integration of the number of photons for each wavelength in the incident light.

■ THE EXPERIMETAL CHARACTERIZATION DATA

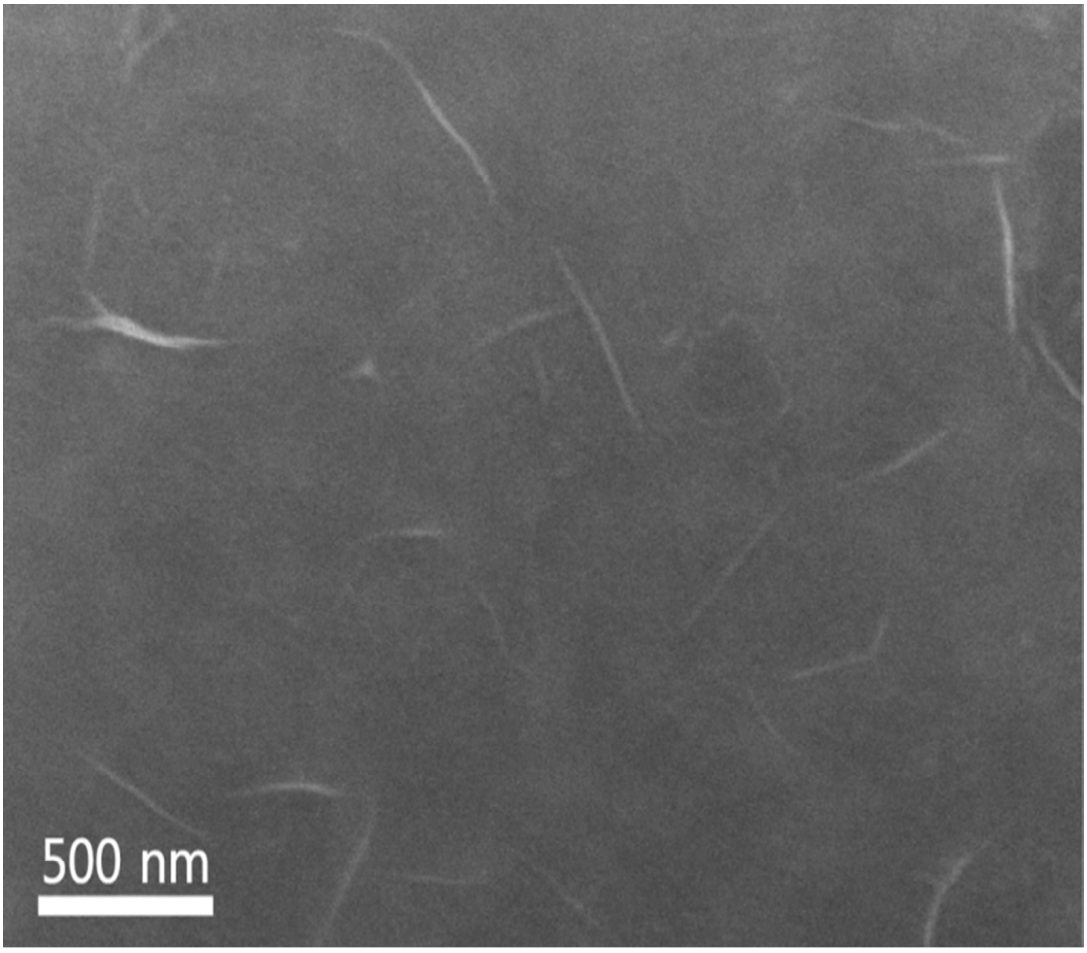

Figure S1. SEM images of the NG film.

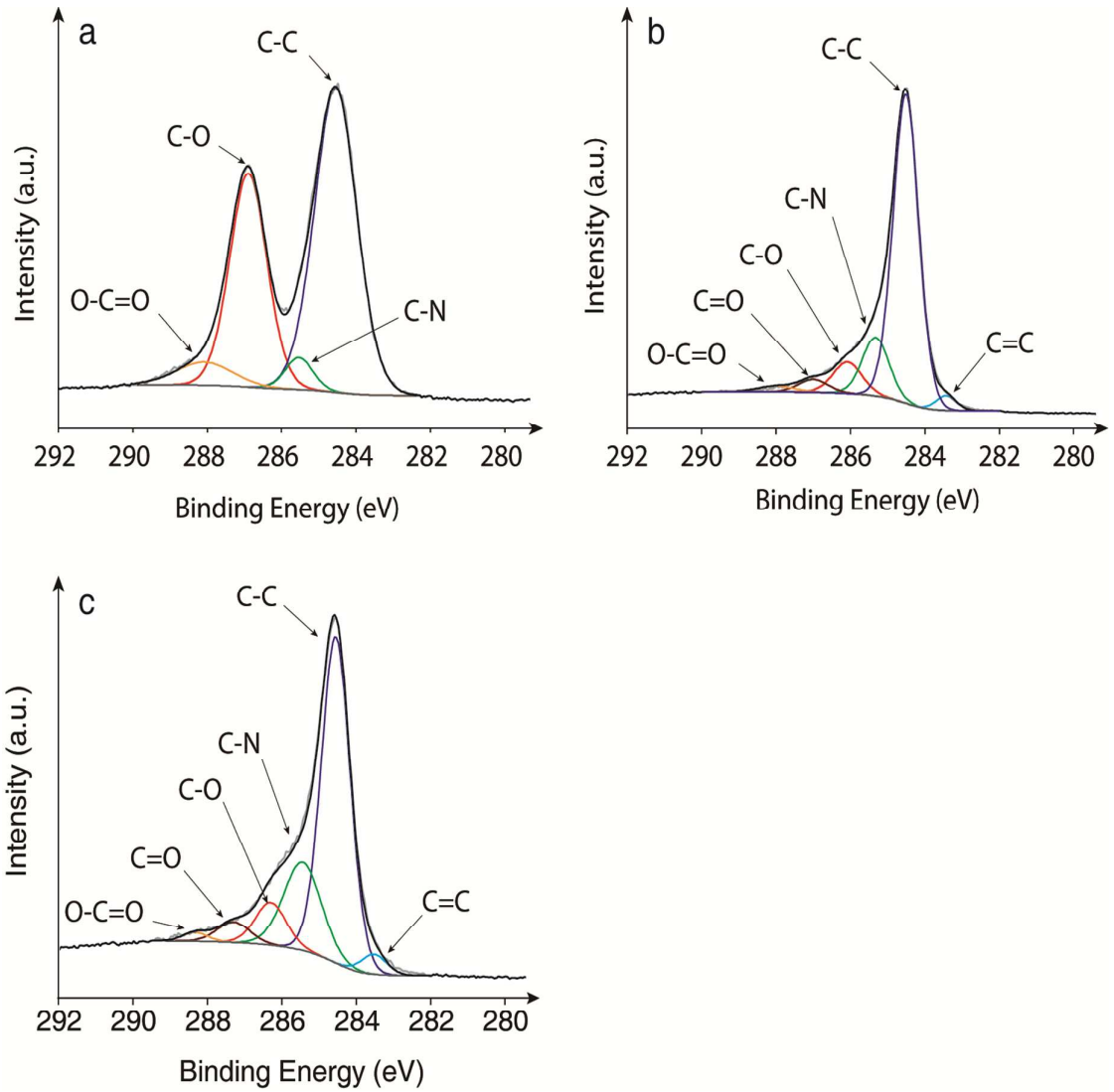

Figure S2. C1s atomic binding configurations (obtained by XPS, Shirley background, Chi-square fit test $< \chi^2_{0.05}$) of (a) GO, (b) RGO and (c) NG.

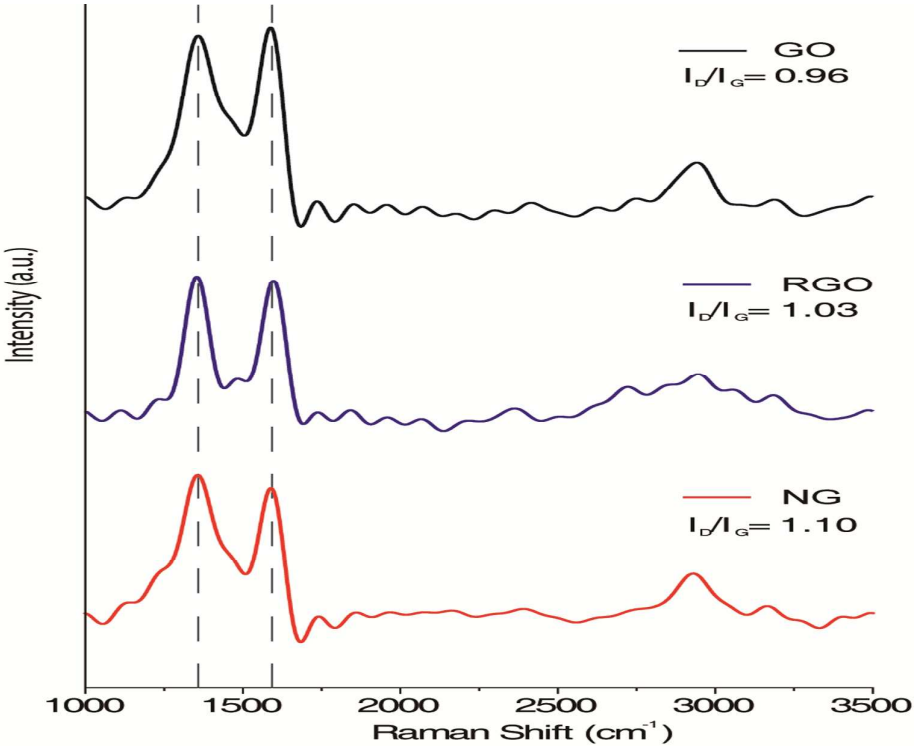

Figure S3. Raman spectra of GO, RGO and NG.

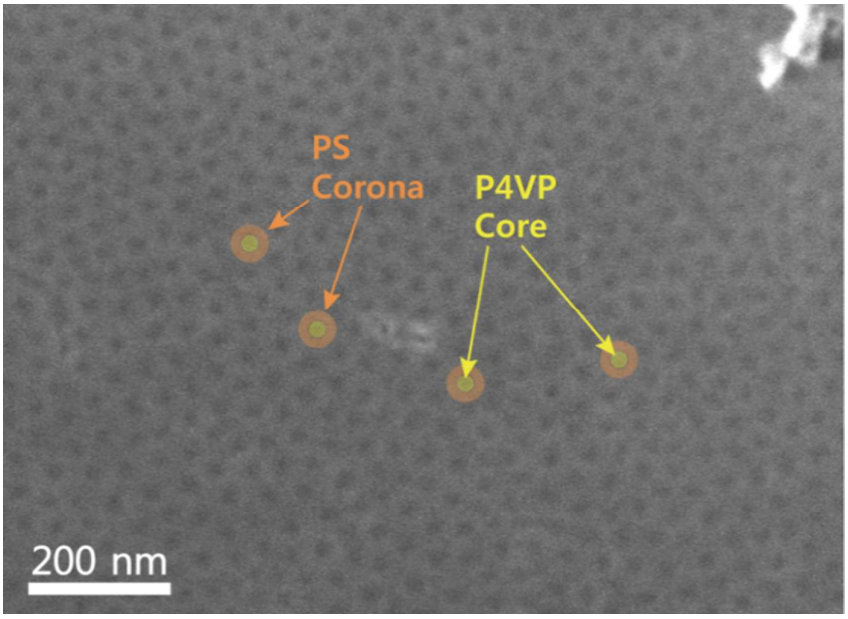

Figure S4. SEM image of the micelle monolayer on the NG.

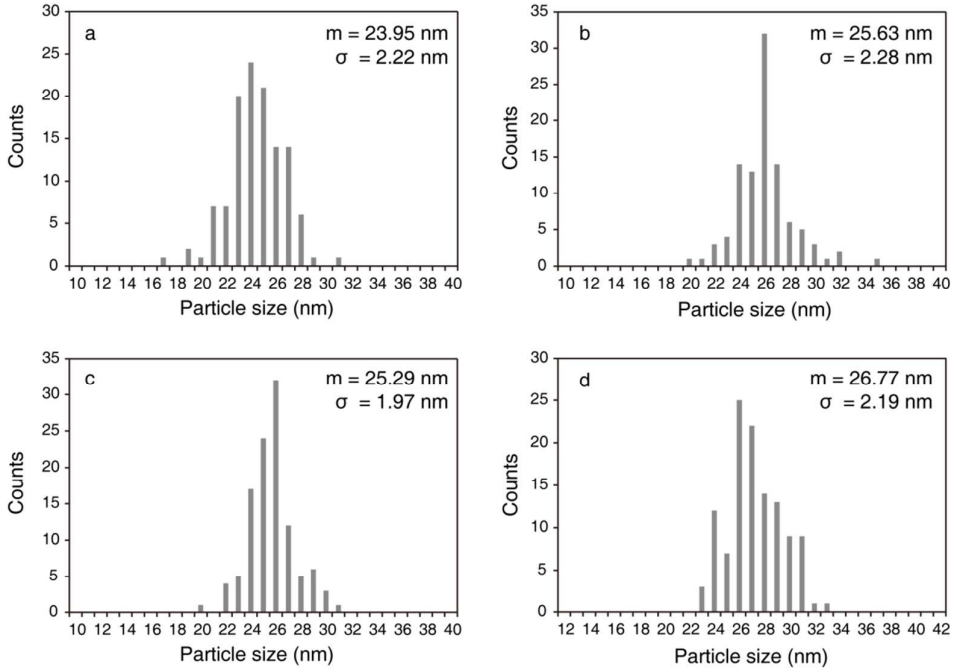

Figure S5. The quantitative size distribution histogram, the average particle size, and the standard deviation (σ) for (a) TiO_2, (b) Cu, (c) Fe, and (d) Pt nanoparticles.

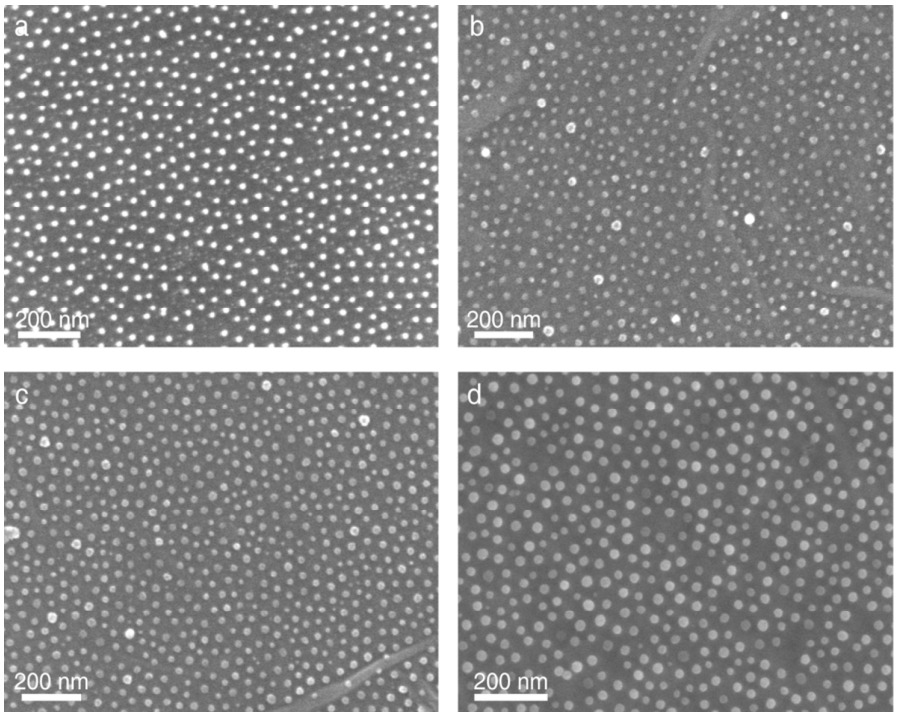

Figure S6. The SEM images of (a) TiO_2-, (b) Cu-, (c) Fe-, and (d) Pt-**on**-NG.

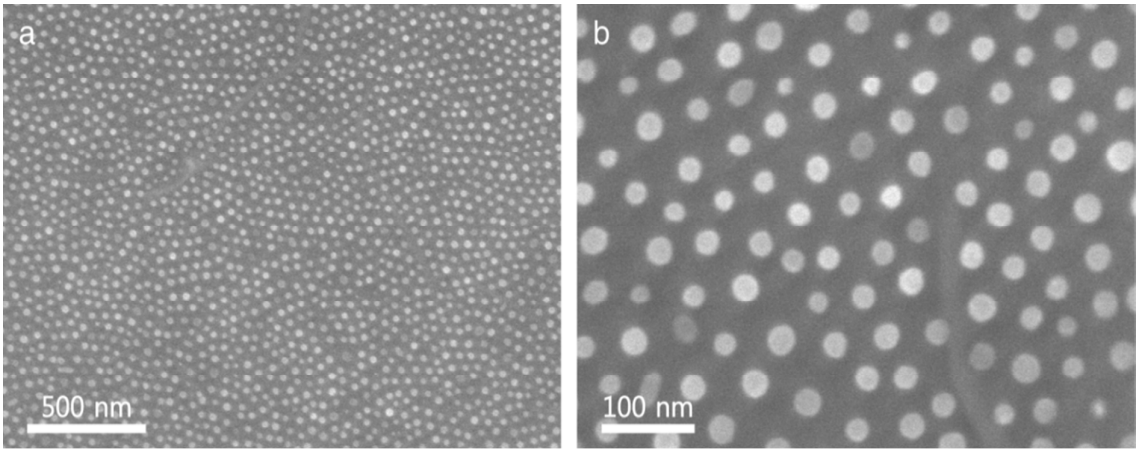

Figure S7. SEM images of ($Pt+TiO_2$)**-on-**NG (a) at a low magnification and (b) a high magnification.

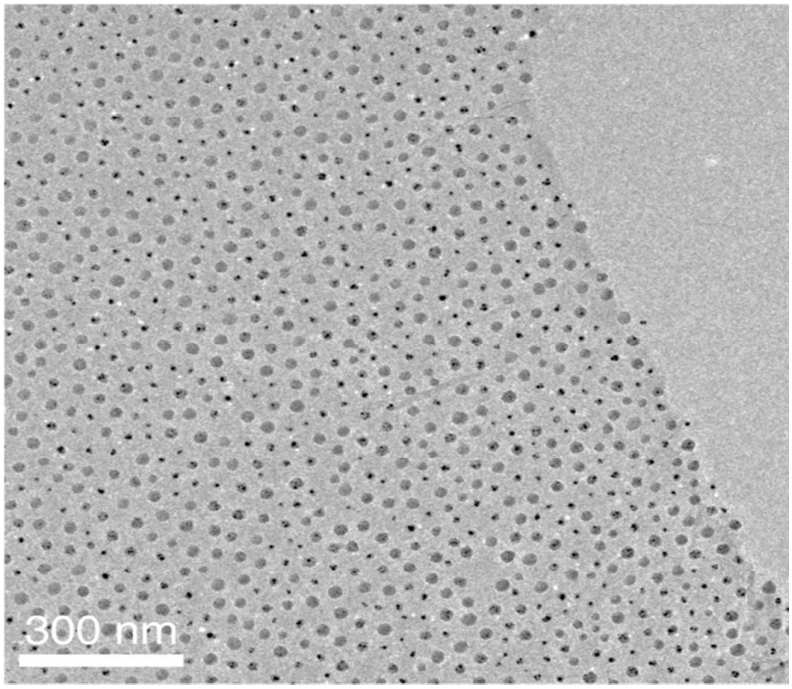

Figure S8. TEM image of ($Pt+TiO_2$)**-on-**NG.

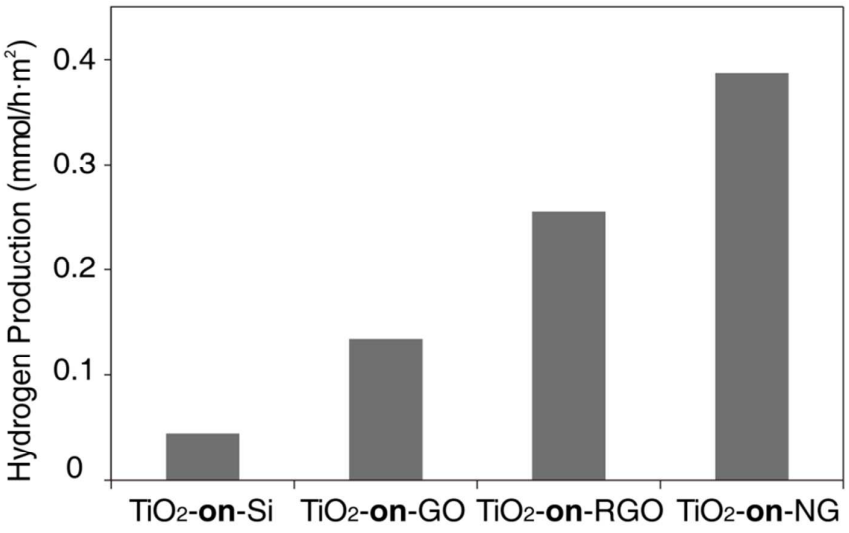

Figure S9. The photocatalytic hydrogen production rates for TiO_2**-on-**Si, TiO_2**-on-**GO, TiO_2**-on-**RGO, and TiO_2**-on-**NG in the irradiation of 24 hrs.

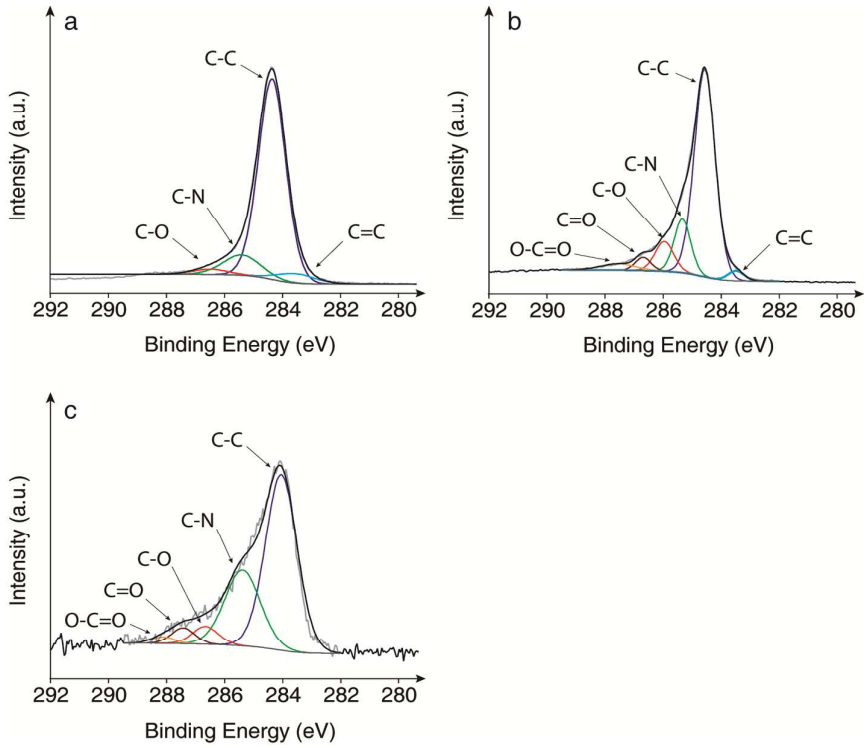

Figure S10. C1s atomic binding configurations (obtained by XPS, Shirley background, Chi-square fit test < $\chi^2_{0.05}$) of three different graphene based materials: (a) GO, (b) RGO, and (c) NG after the photocatalytic reaction for 24 hrs.

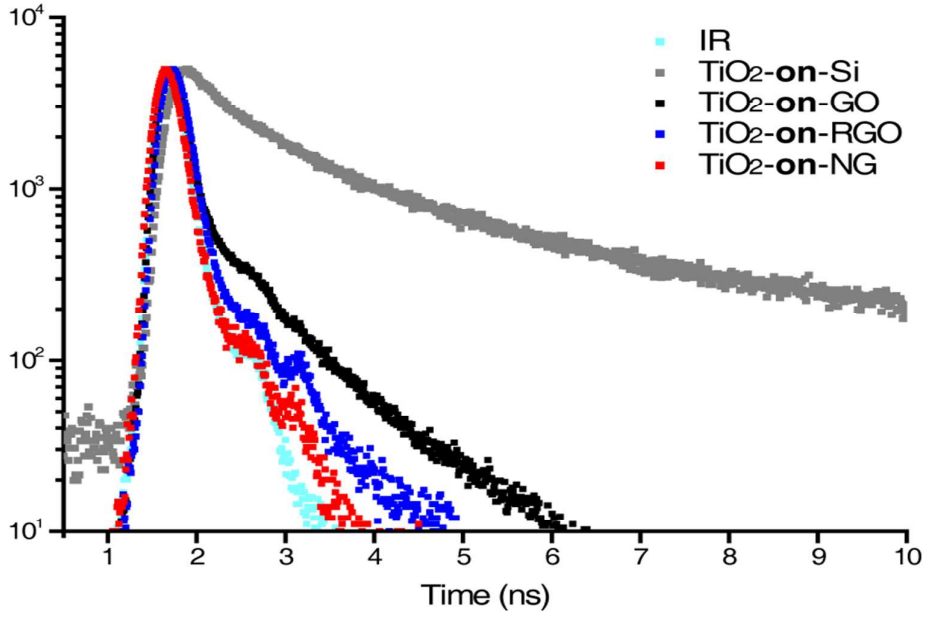

Figure S11. TCSPC fluorescence decay spectra of TiO_2-on-Si –GO, -RGO, and -NG.

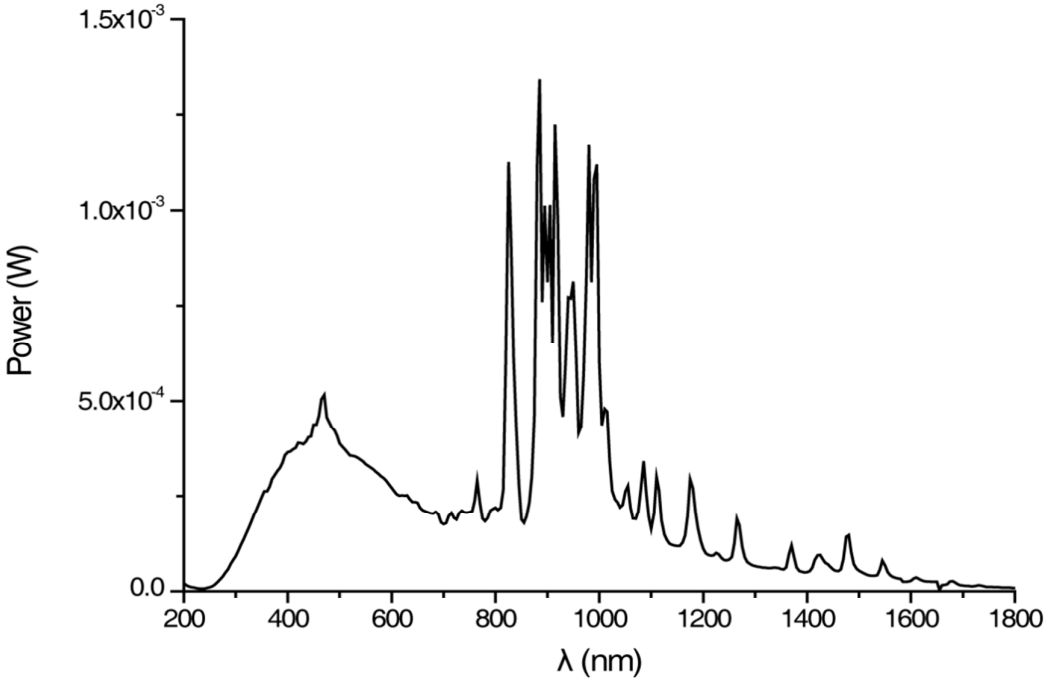

Figure S12. The spectra of the Xe lamp (Newport, Ozone Free Xenon Arc Lamp, 6258).

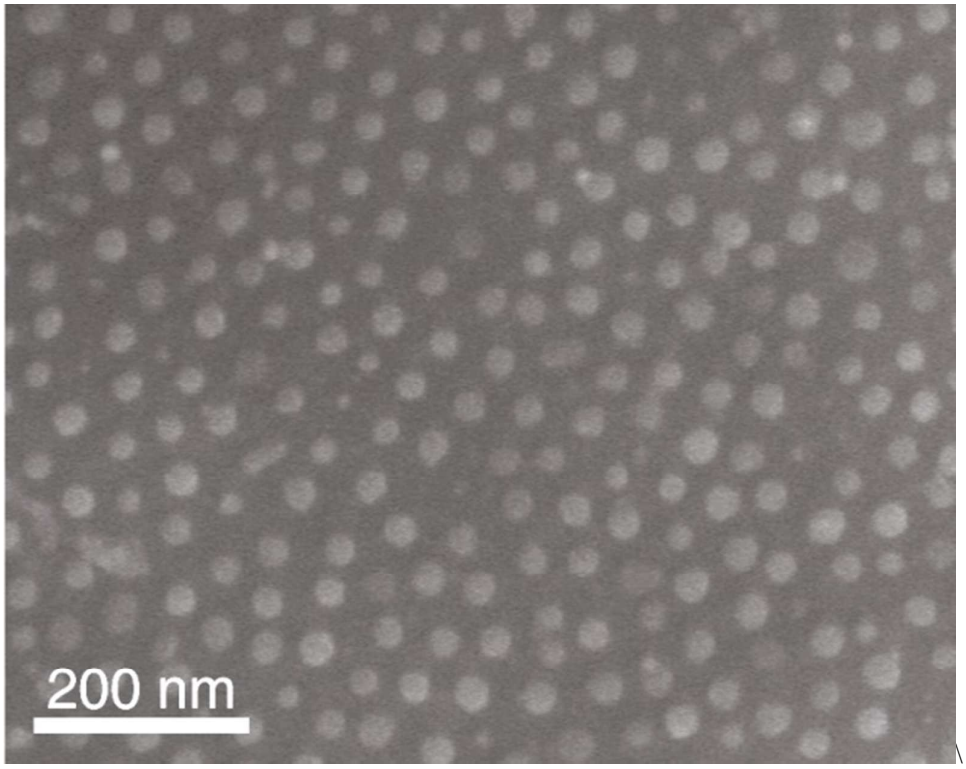

Figure S13. SEM image of ($Pt+TiO_2$)**-on-**NG after the photocatalytic reaction for 24 hrs.

%	GO	RGO	NG
C-C	56.93	70.84	59.02
C-N	2.76	14.02	26.59
C-O	34.76	8.17	3.98

Table S1. C 1s atomic binding configurations of GO, RGO, and NG obtained by the XPS measurements.

%	GO	RGO	NG
C-C	80.73	68.05	60.01
C-N	9.74	13.97	29.17
C-O	5.23	8.77	5.05

Table S2. Chemical compositions of GO, RGO, and NG obtained by the XPS measurements after the photocatalytic reaction for 24 hrs.